



Bolko von Roedern, MS 3212  
National Center for Photovoltaics  
National Renewable Energy Laboratory  
1617 Cole Boulevard  
Golden, CO 80401

07/15/2006

Dear Bolko,

This is the first annual report of our project under the current Thin Film Partnership Program (Subcontract No. XXL-5-44205-12 to University of Nevada, Las Vegas: Characterization of the electronic and chemical structure at thin film solar cell interfaces). A brief summary and details of our activities are given below. This report is in fulfillment of the deliverable schedule of the subcontract statement of work (SOW).

### **Summary**

This project is devoted to deriving the electronic structure of interfaces in  $\text{Cu(In,Ga)(S,Se)}_2$  and  $\text{CdTe}$  thin film solar cells. By using a unique combination of spectroscopic methods (photoelectron spectroscopy, inverse photoemission, and X-ray absorption and emission) a comprehensive picture of the electronic (i.e., band alignment in the valence and conduction band) as well as chemical structure can be painted. The work focuses on (a) deriving the bench mark picture for world-record cells, (b) analyze state-of-the-art cells from industrial processes, and (c) aid in the troubleshooting of cells with substandard performance.

First funds for this project became available in the middle of July 2005. Since then, the workforce of the group was expanded to the size required for this project. The experimental instrumentation at UNLV – a four-chamber ultra-high vacuum surface analysis and modification system – was commissioned and put to routine use after its relocation from the University of Würzburg, Germany. In addition, a setup for inverse photoemission was integrated and a new electron analyzer was installed at UNLV to allow state-of-the-art data acquisition and spectral quality.

Contacts within the Thin Film PV Partnership Program were established to secure a supply of adequate samples. These samples were analyzed both in the lab at UNLV as well as in our beamtimes at the Advanced Light Source, Lawrence Berkeley National Laboratory (Nov. 2 – 13, 2005 and May 16 – 23, 2006).

In our first beamtime within this project at the Advanced Light Source we could

Department of Chemistry  
4505 Maryland Parkway • Box 454003 • Las Vegas, Nevada 89154-4003  
Tel (702) 895-2694 • FAX (702) 895-4072

gather first results with  $\text{Cu(In,Ga)Se}_2$  samples prepared by NREL. Combined with additional photoemission measurements at UNLV, a detailed picture of the chemical composition at several interfaces and surface of the device structure could be drawn. Also during the first beamtime at the Advanced Light Source, we conducted first XES measurements of  $\text{CdTe/CdS}$  samples prepared by the group of A. Compaan (University of Toledo). Recently, these synchrotron results could be complemented by initial photoemission measurements at UNLV of  $\text{CdTe/CdS}$  thin film stacks provided by X. Wu (NREL).

### **Detailed Description of the Activities:**

#### **1. Establishing the workgroup at UNLV**

First funds for this project became available in the middle of July 2005. The initial activity was therefore devoted to the expansion of the work force for this project. With the arrival of Monika Blum, a graduate student from the University of Würzburg, Germany, in late July 2005, of Dr. Marcus Bär, a post-doctoral fellow (recipient of the prestigious German Emmy Noether Scholarship of the Deutsche Forschungsgemeinschaft) in mid-August 2005, and of Dr. Lothar Weinhardt, in January 2006, this expansion was fortunately very fast and successful.

Dr. Bär performed the research for his doctoral thesis at the Hahn-Meitner-Institute in Berlin, Germany, specializing in the optimization of interfaces between novel buffer layer materials and  $\text{Cu(In,Ga)(S,Se)}_2$  thin film solar cell absorbers by chemical surface pretreatments. At UNLV, his primary focus is on modifying interface properties



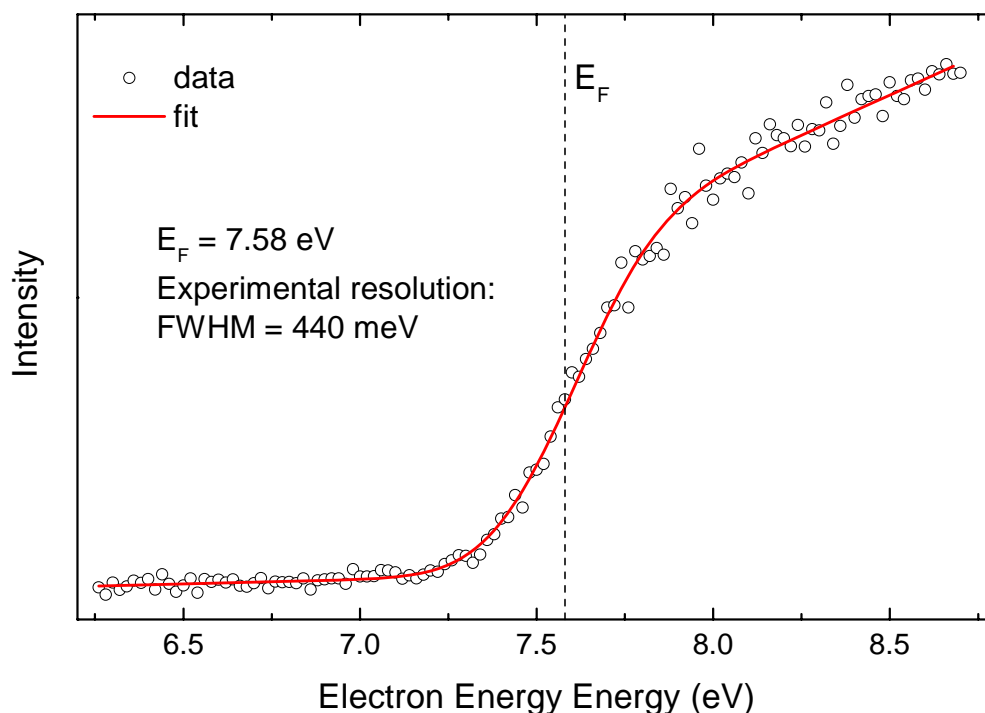
**Fig. 1** Picture of the workgroup in April 2006.

for an optimization of thin film solar cells with wide-gap chalcopyrite absorbers. Dr. Weinhardt, who came from the University of Würzburg, Germany, has pioneered the use of the combination of UV- and Inverse Photoemission for the routine study of band alignment at thin film solar cell interfaces, as well as the to-date least intruding cleaning method for air-exposed thin film chalcopyrite surfaces (50 eV  $\text{Ar}^+$  ion “sputtering”). Both post-docs bring significant expertise in optimization and analysis of surfaces and interfaces in thin film solar cells into this project, and both have published extensively in this area. Monika Blum and Dr. Weinhardt were/are funded through this project. Three undergraduate science majors (John Peiser, Jared White, and Kyle George) from the UNLV Honors College have also joined the group and are involved with this project. Fig. 1 shows a picture of the group in April 2006.

## 2. Commissioning of the four-chamber ultra-high vacuum surface analysis and modification system

The apparatus for the lab experiments at UNLV was successfully commissioned and optimized for routine investigations with X-ray (XPS) and UV (UPS) photoelectron spectroscopy after its relocation from the University of Würzburg, Germany.

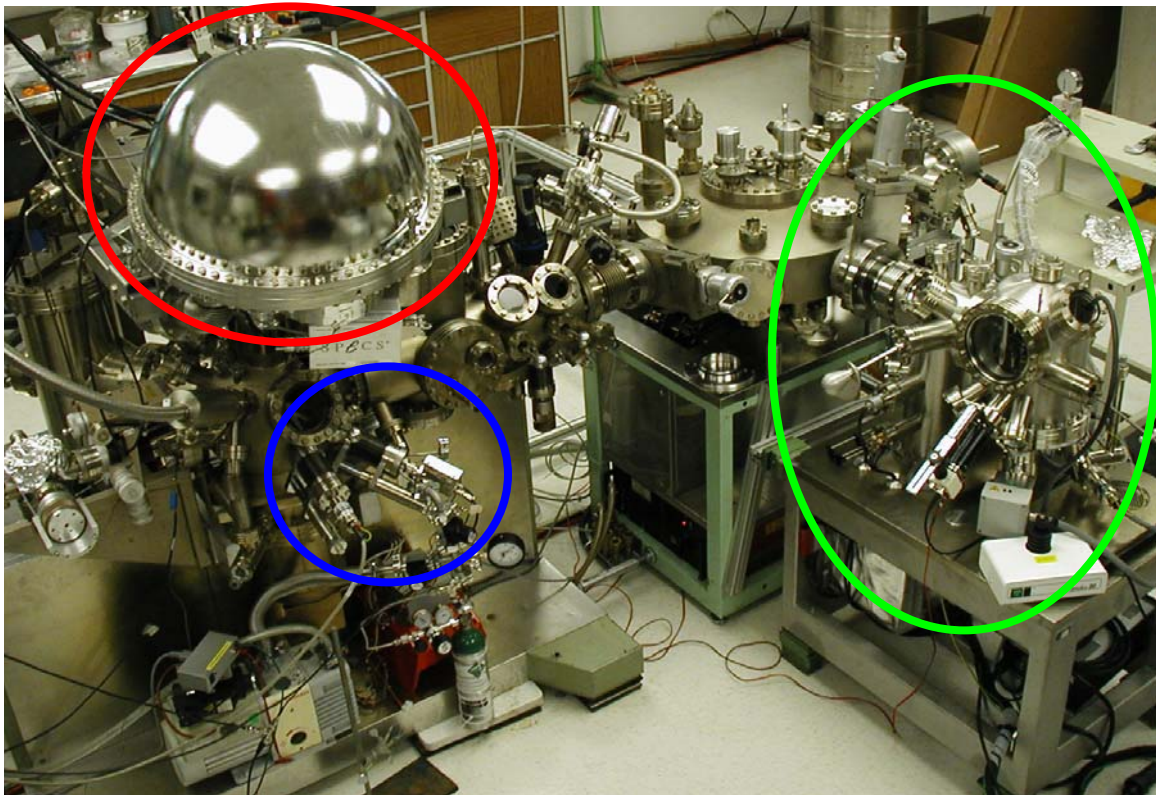
In addition, all necessary items for Inverse Photoemission (IPES), such as a new low-energy/high-current electron gun, a Dose-type photon counter tube, new counting electronics and software, were assembled and installed into the chamber. After arrival of



**Fig. 2** First inverse photoemission spectrum at UNLV (open circles). The red line represents a fit of the experimental data. The derived Fermi energy is given by the dashed vertical line.

the appropriate high-stability, high-voltage power supply in November 2005, first spectra of reference samples were already recorded by the end of 2005. Those spectra are used for a calibration of the absolute energy scale of the setup (i.e, the position of the Fermi energy is measured and used as a reference energy). Fig. 2 shows the first Fermi edge (of a Ag calibration sample) measured with our setup (open circles). The red line represents a fit of the spectrum which is used to derive the Fermi energy and in addition gives us the total energy resolution of our setup (440 meV).

With funds from a different project, we were able to replace the old ESCALab MkII electron analyzer of our surface/interface characterization system, which showed reappearing electronic shortage problems in the first quarter and electronic communication problems in the second and third quarter of this project, by a high-performance state-of-the-art instrument (SPECS PHOIBOS150 MCD) in April 2006. After a downtime of only two weeks the new electron analyzer was commissioned and put to normal operation. The increased spectral resolution and an improvement of the signal-to-noise ratio in XPS by about two orders of magnitude greatly benefits the XPS and UPS results of our project and significantly reduces the experiment times. A picture of the instrument after installation of IPES and replacing the electron analyzer is shown in Fig. 3.



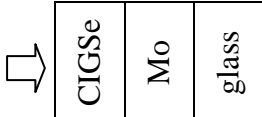
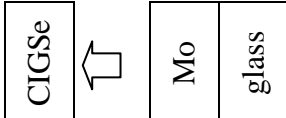
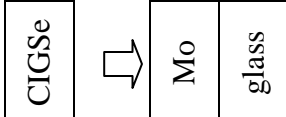
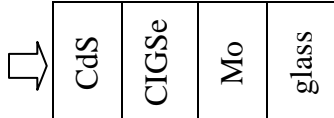

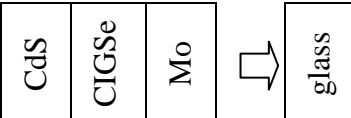
**Fig. 3** Picture of the four-chamber ultra-high vacuum surface modification and analysis instrument at UNLV. Red: replacement electron analyzer; blue: inverse photoemission setup, green: scanning probe microscope.



### 3. Experimental Results

#### A. Investigation of Cu(In,Ga)Se<sub>2</sub> thin films from NREL

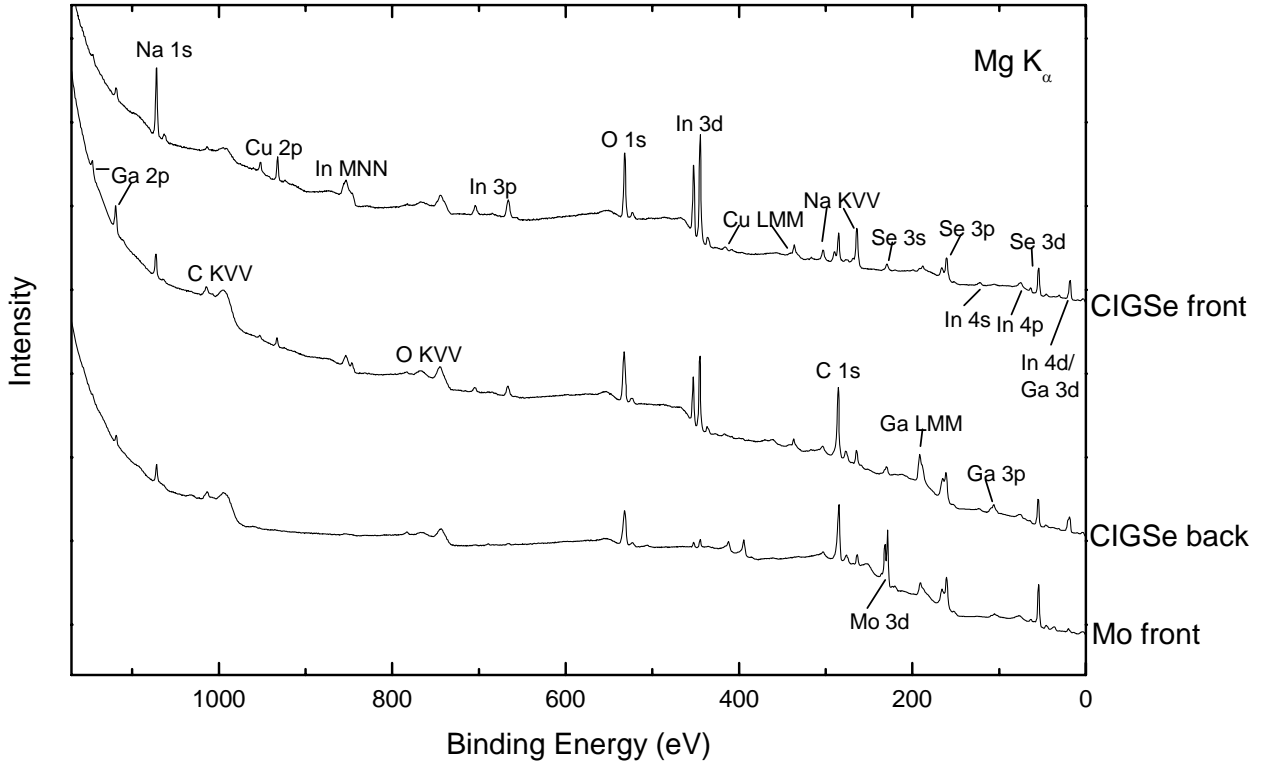
In our beamtime at the Advanced Light Source, Lawrence Berkeley National Laboratory from Nov. 2 – 13, 2005 we could gather first results with Cu(In,Ga)Se<sub>2</sub> (CIGSe) samples prepared by Kannan Ramanathan at NREL. These investigations were based on two different samples, namely CIGSe/Mo/glass and CdS/CIGSe/Mo/glass. To investigate also the interfaces buried beneath the absorber, namely the CIGSe/Mo interface and the Mo/glass interface, we prepared additional samples by cleaving the samples at those interfaces. For doing so, we have glued the front side of both samples to stainless steel plates and divided the stack into two parts. For the CIGSe/Mo/glass sample this cleavage takes place at the CIGSe/Mo-interface, as our measurements show. In contrast, the adhesion between Mo back contact and glass substrate was very weak for the investigated CdS/CIGSe/Mo/glass sample, such that this sample was cleaved at the Mo/glass interface. In total we thus had six different samples (the arrows show the direction of measurement):

Sample	Name in the text	scetch
CIGSe/Mo/glass	CIGSe front	
CIGSe/Mo/glass cleaved, top part	CIGSe back	
CIGSe/Mo/glass cleaved, bottom part	Mo front	
CdS/CIGSe/Mo/glass	CdS	
CdS/CIGSe/Mo/glass cleaved, top part	Mo back	
CdS/CIGSe/Mo/glass cleaved, bottom part	Glass front	

All samples were investigated by X-ray emission spectroscopy (XES) and the first three in the list also by X-ray photoelectron spectroscopy (XPS). Both techniques provide detailed information about the chemical properties of the investigated samples and complement each other with respect to their information depth (XES: bulk sensitive with an

information depth of a few 100 nm, depending on the investigated line; XPS: surface sensitive with an information depth of a few nm).

Fig. 4 shows the XPS survey spectra of the CIGSe front, the CIGSe back and the Mo front. The names chosen for those samples are confirmed by those very surface sensitive spectra, since Mo is only found on the “Mo front” sample called and not on the “CIGSe back” sample.



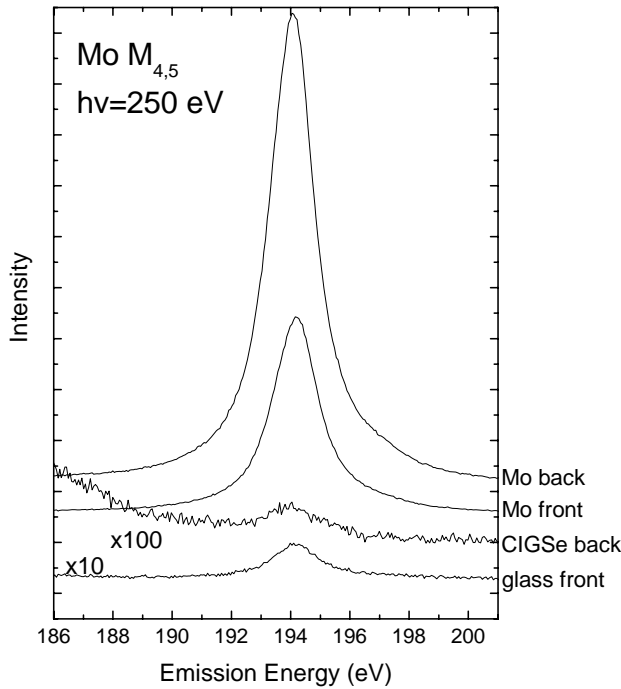
**Fig. 4** XPS survey spectra of the CIGSe front, the CIGSe back, and the Mo front of a Cu(In,Ga)Se<sub>2</sub> NREL absorber.

Since the samples were inevitably exposed to air prior to the measurements, a contamination layer consisting of C and O compounds is formed on their surface, complicating an exact quantitative analysis of the peak intensities. However, quite some qualitative information can be gathered from the XPS survey spectra shown in Fig. 4.

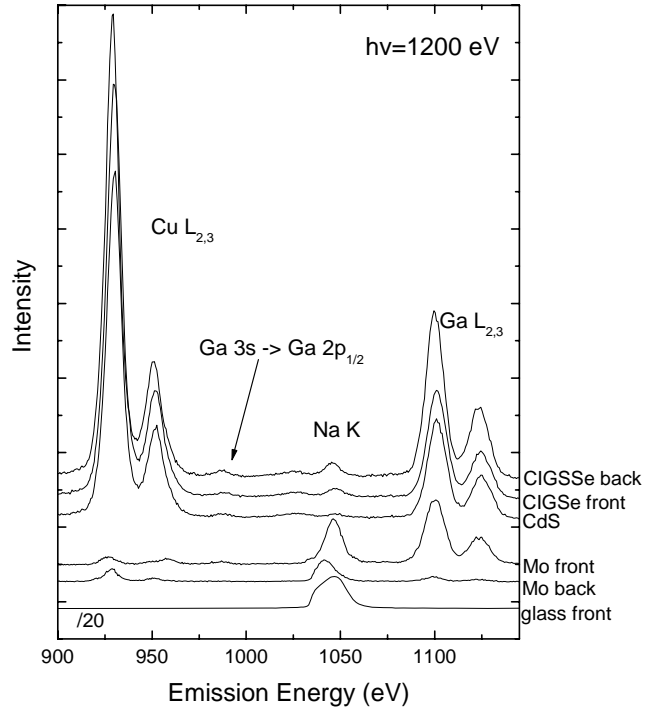
We find that the In 3d signal is stronger on the CIGSe front than on the CIGSe back side. This is because a higher amount of In is replaced by Ga at the absorber back side, which can be seen from the stronger Ga 2p signal at the absorber back side.

The Na amounts on the three samples differ strongly. The highest Na content is found on the absorber front side, whereas much less Na is located around the CIGSe/Mo interface represented by the two other samples.

We find strong indications for different intermixing processes at the CIGSe/Mo interface, as will be discussed in the following. While only trace amounts of In and (within the detection limit of the experiment) no Cu is found, the Se signal increases at



**Fig. 5** Mo  $M_{4,5}$  XES spectra of Mo back, Mo front, CIGSe back, and glass front



**Fig. 6** Cu  $L_{2,3}$ , Na K, and Ga  $L_{2,3}$  spectra of all investigated samples.

the Mo front side, pointing towards the formation of a  $\text{MoSe}_2$  compound, as was found before for  $\text{Cu(In,Ga)(S,Se)}_2$  absorbers [1]. This finding is corroborated by the Mo  $M_{4,5}$  XES spectra shown in Fig. 5. Here the  $M_{4,5}$  emission of the Mo front side is compared with that of the Mo back side (note that the spectra of the CIGSe back and the glass front only show some small Mo remainders). In accordance with the assignment to  $\text{MoSe}_2$  (with a smaller Mo density than in metal Mo) the Mo signal is much weaker at the Mo front side.

Besides the Se diffusion, also a Ga diffusion into the back contact can be observed, which is manifested in the Ga 2p signal seen in the XPS survey spectrum of the Mo front side in Fig. 4. The more bulk sensitive XES measurements (mean free path of around 200 nm for energies around 1000 eV) in Fig. 6, where the Cu  $L_{2,3}$ , Na K, and Ga  $L_{2,3}$  emission was recorded in one energy window, show that this Ga diffusion is very strong. While only small amounts of Cu can be found on the Mo front, the Ga  $L_{2,3}$  intensity is more than half of that on the CIGSe back. The high Ga  $L_{2,3}$  intensity found in the spectrum of the CIGSe back reveals that the Ga content at the CIGSe back compared to the CIGSe front is not only higher at those surfaces but in the whole surface near region.

From the Na K emission lines in Fig. 6, additional information about the Na distribution can be derived. The strongest Na signal is found on the soda lime glass substrate, as expected. In contrast to the surface sensitive measurements above, the Na signal at the CIGSe back is stronger than that at the CIGSe front, which can be explained as follows. It is known that Na at the CIGSe front is mainly localized at its surface and only small amounts are found in the bulk or at grain boundaries near the front surface [2]. This local-

ized Na gives a strong signal in the surface sensitive XPS measurements, whereas the Na content in the bulk and at grain boundaries next to the surface plays a more important role for the XES spectra. Therefore, the higher Na signal in the Na K XES spectra can be attributed to a higher Na content in the bulk region next to the back contact and/or at grain boundaries next to the CIGSe back.

It is planned to continue the investigations described above and extend them by investigating customized sample series with UPS and IPES to get insight into the band alignments at the various interfaces of the NREL-CIGSe device structure.

## B. XES-investigation of CdTe/CdS samples from Univ. Toledo

Also during beamtime at the Advanced Light Source, Lawrence Berkeley National Laboratory, we conducted first XES measurements of CdTe/CdS samples prepared by the group of A. Compaan (University of Toledo). These investigations were based on two sets of samples, namely differently treated CdS thin films and CdTe/CdS thin film stacks, respectively. For the latter set of samples, the impact of CdCl<sub>2</sub>-treatment on the CdTe/CdS thin film stacks was investigated, while for the CdS thin films also the influence of Cu-diffusion was analyzed. In addition, some powder samples (CdS, CdSO<sub>4</sub>, CdCl<sub>2</sub>) were characterized for comparison.

In total, we thus investigated eight different samples:

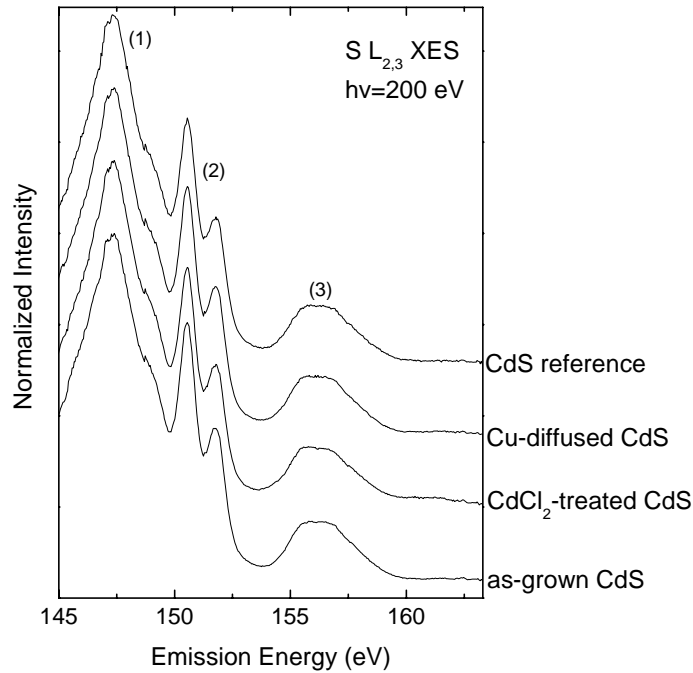
Sample	Treatment	Name in the text
CdS (thin film on glass)	none	as-grown CdS
CdS (thin film on glass)	CdCl <sub>2</sub> -treated	CdCl <sub>2</sub> -treated CdS
CdS (thin film on glass)	Cu-diffused	Cu-diffused CdS
CdTe/CdS (thin film stack on glass)	none	as-grown CdTe/CdS
CdTe/CdS (thin film stack on glass)	CdCl <sub>2</sub> -treated	CdCl <sub>2</sub> -treated CdTe/CdS
CdSO <sub>4</sub> , CdS, CdCl <sub>2</sub> (powders)	N/A	CdSO <sub>4</sub> , CdS, CdCl <sub>2</sub> references



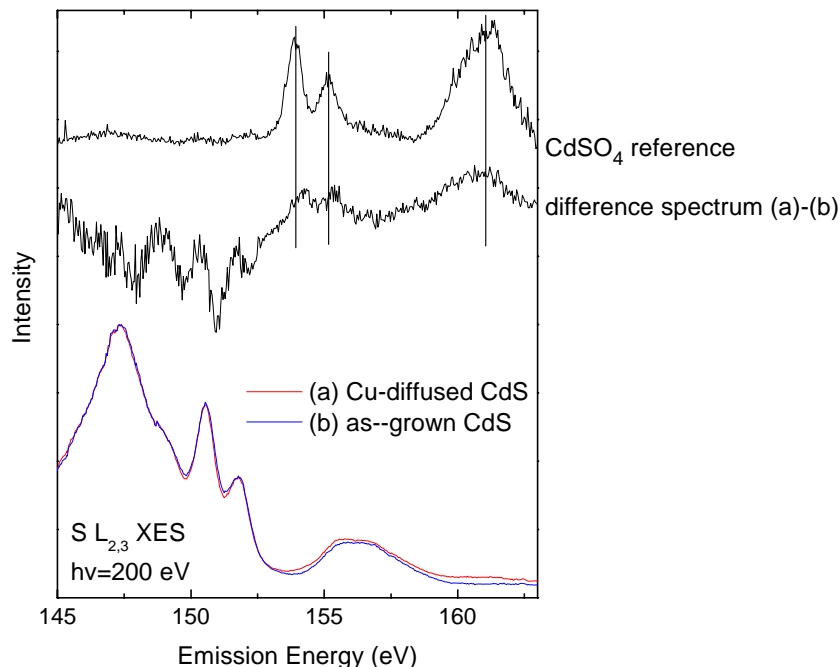
All samples were investigated by X-ray emission spectroscopy (XES). As mentioned above, this technique provides detailed information about the chemical properties of the investigated samples, and, as a photon-in photon-out technique, probes the “near-surface” bulk. In our case, where we have focused on the S  $L_{2,3}$  and Cl  $L_{2,3}$  emission, XES has an information depth of about 100 nm.

Fig. 7 shows the S  $L_{2,3}$  XES spectra of the set of CdS samples. At first sight, all spectra look identical. The main feature (1) at 147.3 eV (which is actually a doublet indicated by the clearly visible shoulder at 149 eV) can be ascribed to S 3s electrons decaying into S  $2p_{1/2}$  and S  $2p_{3/2}$  core holes. In addition, the two peaks at 150.5 eV and 151.8 eV (2) correspond to Cd 4d electrons decaying into the S  $2p_{1/2}$  and S  $2p_{3/2}$  core holes, respectively, and thus indicate sulfur atoms bound to Cd. Furthermore, we observe the upper valence band of CdS at about 156 eV. Altogether, all spectra show the typical features of a S  $L_{2,3}$  spectrum of CdS, which is also confirmed by the respective spectrum of the CdS reference. However, a close inspection of the data shows small but significant differences for, e.g., the S  $L_{2,3}$  XES spectrum of the as-grown CdS (a) compared to that of the Cu-diffused CdS sample (b), as shown in Fig. 8. In Fig. 8, the raw spectra and the corresponding difference spectrum are shown. The comparison of the (enlarged) difference (a)-(b) with a CdS and a CdSO<sub>4</sub> reference spectrum reveals that the features in the difference spectrum can be ascribed to the formation of S-O bonds and a localization of the Cd 4d-derived band.

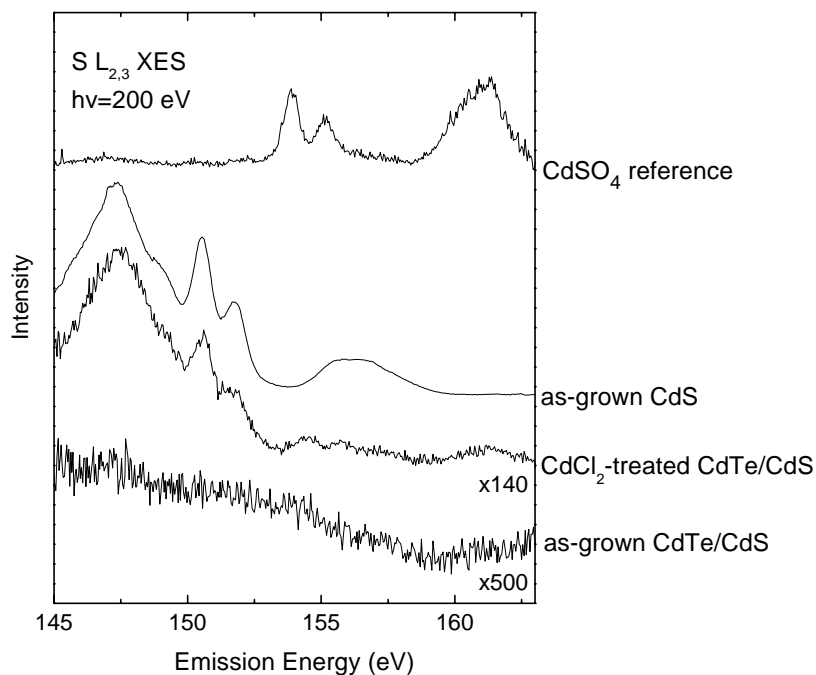
The spectra of the differently treated CdTe/CdS thin film stacks are shown in Fig. 9. Since the thickness of the CdTe layer, which covers the CdS, is significantly beyond the information depth of XES, one would not expect to observe a S  $L_{2,3}$  signal. This is indeed the case for the as-grown CdTe/CdS thin film stack. However, the S  $L_{2,3}$  spectrum



**Fig. 7** S  $L_{2,3}$  XES spectra of a set of differently treated CdS thin films. In addition, a corresponding spectrum of a CdS reference is also shown (top spectrum). The main features are labeled (1) – (3).



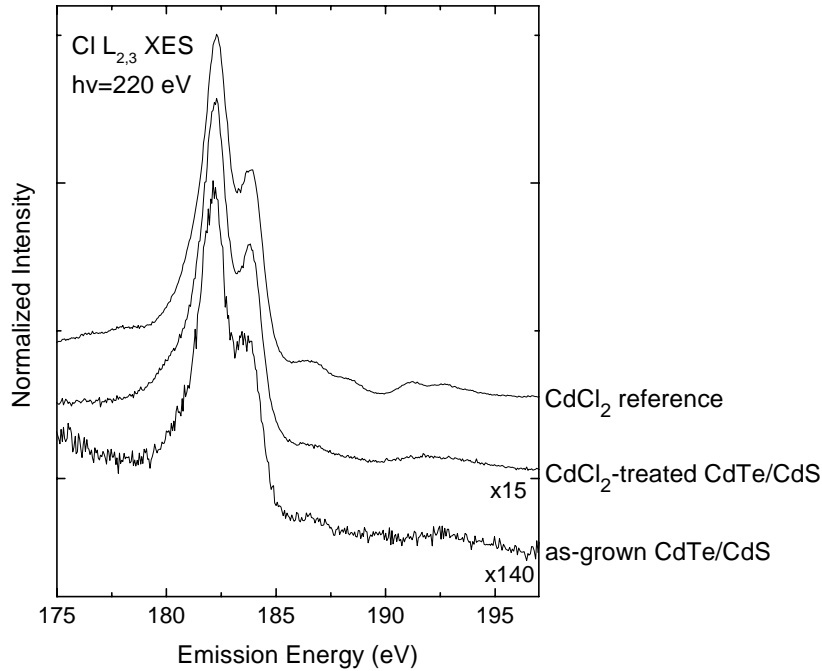
**Fig. 8** S  $L_{2,3}$  XES spectra of a Cu-diffused CdS thin film (a) plotted upon that of an as-grown CdS sample (b). In addition, the corresponding (enlarged) difference spectrum (a-b) and a  $\text{CdSO}_4$  reference spectrum is also shown.



**Fig. 9** S  $L_{2,3}$  XES spectra of a set of differently treated CdTe/CdS thin film stacks. In addition, the corresponding spectrum of an as-grown CdS thin film and a  $\text{CdSO}_4$  reference spectrum are also shown. Note the different magnification factors.

of the  $\text{CdCl}_2$ -treated  $\text{CdTe/CdS}$  sample clearly shows some small (note the magnification factor) spectral features, which are similar to the  $\text{CdS}$  spectra shown in Fig. 7. A comparison with the spectrum of the as-grown  $\text{CdS}$  thin film as well as with the  $\text{CdSO}_4$  reference reveals that the  $\text{S L}_{2,3}$  spectrum of the  $\text{CdCl}_2$ -treated  $\text{CdTe/CdS}$  thin film stack can be described as a superposition of spectral features of both reference samples. Most prominently, the two peaks at 150.5 eV and 151.8 eV directly indicate S-Cd bonds, and the peaks at 153.9 eV, 155.1 eV, and 161.0 eV can be directly ascribed to S-O bonds. In consequence, this points to a  $\text{CdCl}_2$ -treatment-induced crack or void formation of the  $\text{CdTe}$  layer or, more likely, to a strong intermixing (the latter is commonly accepted in the community). For the  $\text{CdTe/CdS}$  thin film stacks we also investigated the  $\text{Cl L}_{2,3}$  XES spectra, as shown in Fig. 10 (multiplied by the given magnification factors). The two major features of the observed spectra at 182.3 eV and 183.8 eV can again be ascribed to 3s electrons decaying into the  $2p_{1/2}$  and  $2p_{3/2}$  core holes, this time for electrons in Cl. As expected, we find a  $\text{Cl L}_{2,3}$  XES spectrum for the  $\text{CdCl}_2$ -treated  $\text{CdTe/CdS}$  sample (middle spectrum in Fig. 10), the main features of which are quite similar to those of the  $\text{CdCl}_2$  reference. The fact that the structures between 185 and 190 eV and between 190 eV and 194 eV are less pronounced than in the reference sample, indicates the presence of Cl atoms that are not directly bound to Cd. Surprisingly, one can also identify a weak (note the magnification factor)  $\text{Cl L}_{2,3}$  XES spectrum for the as-grown  $\text{CdTe/CdS}$  thin film stack, which shows all the characteristics of  $\text{CdCl}_2$ . Whether this is due to extrinsic contamination or an result of the used sample preparation (and thus significant) is the topic of future experiments.

Based on these results, we will continue the investigation of these  $\text{CdTe/CdS}$



**Fig. 10**  $\text{Cl L}_{2,3}$  XES spectra of a set of differently treated  $\text{CdTe/CdS}$  thin film stacks. In addition, the corresponding spectrum of  $\text{CdCl}_2$  reference spectrum is also shown. Note the different magnification factors.

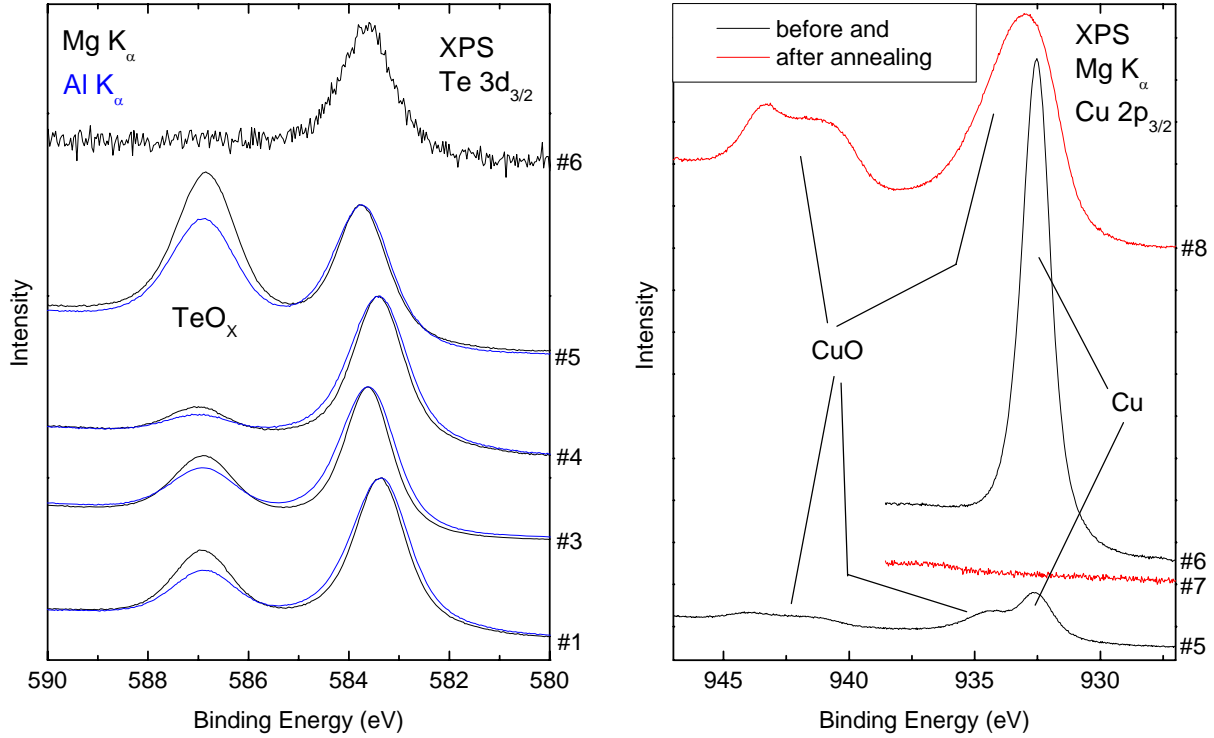
samples and extend them by investigating customized sample series with UPS and IPES to get insight into the band alignments at the various interfaces of the device structure of the CdTe-based solar cell.

### C. PES-investigation of CdTe/CdS samples from NREL

In order to become familiar with the special characteristics of CdTe/CdS samples with respect to their investigation in photoemission measurements, we conducted first XPS measurements of CdTe/CdS samples prepared by the group of X. Wu (NREL). The first set of test structures consisted of the following samples:

Sample	Treatment	Name in the text
CdTe/CdS (thin film stack on glass)	none	#1
CdTe/CdS (thin film stack on glass)	CdCl <sub>2</sub> -treated and etched	#3
CdTe/CdS (thin film stack on glass)	CdCl <sub>2</sub> -treated	#4
Cu (5nm)/CdTe/CdS (thin film stack on glass)	Before Cu deposition: CdCl <sub>2</sub> - treated and etched After Cu deposition: None	#5
Cu (150nm)/CdTe/CdS (thin film stack on glass)	Before Cu deposition: CdCl <sub>2</sub> - treated and etched After Cu deposition: None	#6
Cu (5nm)/CdTe/CdS (thin film stack on glass)	Before Cu deposition: CdCl <sub>2</sub> - treated and etched After Cu deposition: Anneal- ing for 30s @ 250°C	#7
Cu (150nm)/CdTe/CdS (thin film stack on glass)	Before Cu deposition: CdCl <sub>2</sub> - treated and etched After Cu deposition: Anneal- ing for 30s @ 250°C	#8

In view of the high surface sensitivity of XPS, all samples showed significant surface contamination (see discussion below), prohibiting a meaningful subsequent characterization by UPS or IPES. However, there is evidence that the contamination (oxidation) is concentrated at the surface, most likely caused by exposing the samples to ambient air. This indicates that with proper sample handling and, possibly, a low-energy (50 eV) ion desorption step, sufficiently clean surfaces can be obtained. The fact that Te is indeed only oxidized at the sample surface is confirmed by the Te 3d<sub>3/2</sub> spectra shown in Fig. 11 (left). All spectra show a significant high binding energy feature at approx. 587 eV, indicative for oxidized tellurium, except the corresponding spectrum of sample #6. Here,



**Fig. 11** Detail spectra of the Te 3d<sub>3/2</sub> (left) and Cu 2p<sub>3/2</sub> (right) photoemission line of the different investigated CdTe/CdS thin film stacks.

the tellurium is covered by a thick [nominal 150 nm] Cu layer preventing its oxidation. (Note that a tellurium XPS-signal is visible “through” the thick Cu layer, which is a strong indication that the Cu does not cover the underlying CdTe completely.) The “buried” non-oxidized tellurium indicates that the oxidation takes place after the actual production process. Furthermore, the graph shows the Te 3d<sub>3/2</sub> photoelectrons not only excited with Mg K<sub>α</sub> ( $h\nu = 1253.6$  eV) but also with Al K<sub>α</sub> excitation ( $h\nu = 1486.6$  eV). Using Al K<sub>α</sub> excitation, the electrons have a higher kinetic energy and thus according to the “universal curve” of the inelastic mean free path (IMFP) [3] a larger IMFP. Therefore, the corresponding spectra (Fig. 11 (left), blue) are less surface sensitive. It can be observed that the intensity of the TeO<sub>x</sub> component (high binding energy feature) in those spectra is smaller as compared to that of the respective spectra conducted with Mg K<sub>α</sub> excitation, also confirming that the tellurium is only oxidized at the sample surface.

An additional interesting result is shown in Fig. 11, right. While sample #6 (thick [nominal 150nm] Cu layer on the CdTe/CdS stack) shows metallic Cu, the very thin [nominal 5nm] Cu film of sample #5 is partly oxidized, as indicated by a second peak at higher binding energies around 943 eV. The spectra clearly show the presence of CuO, since, for Cu<sub>2</sub>O, the peak would only be shifted by ~1 eV to higher binding energies with respect to the Cu 2p<sub>3/2</sub> photoemission line of metallic Cu. Furthermore, for CuO two peaks as observable in the present case are typical. In addition, it can be observed that after annealing of the Cu/CdTe/CdS thin film stacks the thin Cu layer is vanished (com-

pare spectra of samples #5 and #7 Fig. 11, right) and the thick Cu layer is also partly oxidized (compare spectra of samples #6 and #8 Fig. 11, right), respectively.

- [1] L. Weinhardt, O. Fuchs, A. Peter, E. Umbach, C. Heske, J. Reichardt, M. Bär, I. Lauermann, I. Kötschau, A. Grimm, S. Sokoll, T.P. Niesen, S. Visbeck, and F. Karg, *J. Phys. Chem.* **124**, 074705 (2006).
- [2] C. Heske, D. Eich, R. Fink, E. Umbach, T. van Buuren, C. Bostedt, S. Kakar, L. J. Terminello, M. M. Grush, T. A. Callcott, F. J. Himpsel, D. L. Ederer, R. C. C. Perera, W. Riedl, and F. Karg, *Surf. Interface Anal.* **30**, 459 (2000).
- [3] D. Briggs and M.P. Seah, *Practical Surface Analysis by Auger and X-ray photoelectron spectroscopy*, John Wiley, New York (1983).

### **Project presentations**

- 1. M. Bär, “Formation of the buffer/CuInS<sub>2</sub> interface”, WCPEC-4, Hawaii, May 2006.
- 2. L. Weinhardt, “Unfavorable band alignment at the CdS/Cu(In,Ga)S<sub>2</sub> interface in thin film solar cells”, WCPEC-4, Hawaii, May 2006.
- 3. C. Heske, “Chemical and electronic properties of the CdS/Cu(In,Ga)(S,Se)<sub>2</sub>/Mo junctions in thin film solar cells”, EMRS2006, Nice, France, May 2006.

### **Submitted conference articles (deliverable: one submitted conference article)**

- 1. M. Bär et al., “Chemical Bath Deposition of CdS Thin Films on CuInS<sub>2</sub> and Si substrates – a comparative x-ray emission study”, Proc. WCPEC-4, Hawaii, May 2006.
- 2. L. Weinhardt et al., “Comparison of band alignments at various CdS/Cu(In,Ga)(S,Se)<sub>2</sub> interfaces in thin film solar cells”, Proc. WCPEC-4, Hawaii, May 2006.
- 3. L. Weinhardt et al., “Chemical properties of the Cu(In,Ga)Se<sub>2</sub>/Mo/glass interfaces in thin film solar cells”, Proc. EMRS 2006, Nice, France, May 2006. Submitted to Thin Solid Films.

If you have any questions, please do not hesitate to call me at (702) 895-2694.

Sincerely,

C. Heske  
Associate Professor  
Department of Chemistry  
University of Nevada, Las Vegas

CC: C. Lopez